J. Fluid Mech. (2009), *vol.* 638, *pp.* 161–172. © Cambridge University Press 2009
doi:10.1017/S0022112009991261

A planar pulsating jet

N. RILEY[1]†, M. SÁNCHEZ-SANZ[2] AND E. J. WATSON[3]

[1]School of Mathematics, University of East Anglia, Norwich, NR4 7TJ, UK

[2]ETSI Aeronáuticos, Pl. Cardenal Cisneros 3, 28040 Madrid, Spain

[3]30 Ashwood Avenue, Manchester, M20 2ZB, UK

(Received 4 June 2008; revised 20 July 2009; accepted 21 July 2009)

We are concerned with the behaviour of a two-dimensional jet that issues from a planar orifice, with a 'top-hat' profile. At the orifice the steady flow is modulated by a time-harmonic fluctuation. A suitably defined Reynolds number is assumed to be large throughout. At large streamwise distances from the orifice, the time-averaged flow yields the classical, Bickley, jet with a suitable virtual origin. This decays algebraically whilst, by contrast, the unsteady component decays exponentially with streamwise distance. An asymptotic theory confirms the exponential decay and provides a good agreement with the numerical solution.

1. Introduction

In this paper, we consider the flow in a two-dimensional jet issuing from between plane boundaries a distance $2h$ apart. The onset flow, where the jet issues from the orifice, comprises a steady uniform component U superimposed upon which is a periodic fluctuation of amplitude ϵU and frequency ω. Of particular interest is the nature of the downstream decay of the jet. A Reynolds number $R = Uh/\nu$, where ν is the kinematic viscosity, is assumed to be large so that the unsteady boundary-layer equations result, characterized by the single parameter $S = \omega h^2/\nu$.

In § 2, we present results from an integration of these equations for a particular value of S, and various $O(1)$ values of ϵ. The integration advances the solution in time until a periodic solution emerges. In the absence of the unsteady component ($\epsilon = 0$), the jet develops from its initial 'top hat' form to the self-similar solution (Schlichting 1933; Bickley 1937), as $x \to \infty$, where x is the streamwise variable. In this solution, the axial velocity decays algebraically as $O(x^{-1/3})$ and the jet thickens as $O(x^{2/3})$. For values of $\epsilon \neq 0$, we have found that the disturbance due to the modulation at $x = 0$ decays much more rapidly, and the steady self-similar jet emerges.

In order to gain some understanding of this very rapid decay, we have, in § 3, carried out a perturbation analysis for $\epsilon \ll 1$. The $O(1)$ leading term is the steady jet, which evolves into the self-similar form. At $O(\epsilon)$, the fluctuating perturbation satisfies a linear equation. An analysis of this for large x shows that the unsteady flow domain divides into an outer region of thickness $O(x^{2/3})$, as in the steady case, and an inner region of thickness $O(x^{1/3})$. Matching the inner and outer solutions leads to an eigenvalue problem. The lowest eigenvalue, perhaps unexpectedly, predicts a solution that grows exponentially at large distances downstream. This is clearly not in accord with the results reported in § 2. The second eigenvalue predicts a physically

† Email address for correspondence: N.Riley@uea.ac.uk

https://doi.org/10.1017/S0022112009991261 Published online by Cambridge University Press

and numerically acceptable exponentially decaying solution far downstream. This exponential decay, whose rate of decay increases with S, may be compared with the algebraic decay of the steady jet. Various aspects of the numerical solution for large x are compared with the asymptotic two-layer perturbation solution and a satisfactory agreement is recorded.

2. Governing equations and numerical solution

We are concerned with the flow of an incompressible viscous fluid, for which the governing equations are

$$\frac{\partial \mathbf{v}'}{\partial t'} - \mathbf{v}' \wedge (\nabla \wedge \mathbf{v}') = \frac{1}{\rho}\nabla(p' + \tfrac{1}{2}\rho \mathbf{v}'^2) - \nu \nabla \wedge \nabla \wedge \mathbf{v}', \qquad \nabla.\mathbf{v}' = 0. \tag{2.1}$$

In these equations, t' is the time, $\mathbf{v}' = (u', v')$ is the velocity, p' is the pressure, ρ is the density and ν is the kinematic viscosity of the fluid. A jet is assumed to emerge at $x' = 0$, into fluid otherwise at rest, from the parallel planes $y' = \pm h$, so that at $x' = 0$ the initial conditions are

$$u' = \begin{cases} U(1 + \epsilon \cos \omega t'), & |y'| < h, \\ 0, & |y'| > h, \end{cases} \tag{2.2}$$

where ω is the frequency of the fluctuation and U, ϵ are constants.

If we introduce dimensionless variables such that

$$x = \nu x'/Uh^2, \quad y = y'/h, \quad t = \omega t', \quad u = u'/U, \quad v = v'h/\nu \quad \text{and} \quad p = p'/\rho U^2,$$

then for Reynolds number $R = Uh/\nu \gg 1$, the pressure is uniform across the jet and the x-component of (2.1) and the continuity equation, become

$$S\frac{\partial u}{\partial t} + u\frac{\partial u}{\partial x} + v\frac{\partial u}{\partial y} = \frac{\partial^2 u}{\partial y^2}, \qquad \frac{\partial u}{\partial x} + \frac{\partial v}{\partial y} = 0, \tag{2.3}$$

where $S = \omega h^2/\nu$ is the Stokes number. The initial condition (2.2) is now, at $x = 0$,

$$u = \begin{cases} 1 + \epsilon \cos t, & |y| < 1, \\ 0, & |y| > 1. \end{cases} \tag{2.4}$$

The remaining boundary conditions for (2.3) require

$$\left.\begin{aligned} &v = \partial u/\partial y = 0 \quad \text{at} \quad y = 0, \quad x > 0, \\ &u \to 0 \quad \text{as} \quad y \to \infty, \quad x > 0. \end{aligned}\right\} \tag{2.5}$$

We have addressed, numerically, the equations (2.3) together with the onset condition (2.4) and the boundary conditions (2.5). To enable this, we have used a fully implicit second-order accurate marching procedure in both time t and the streamwise direction x, using backward finite-difference formulae and standard second-order accurate central differences for the transverse derivatives. Uniform grids in time and the streamwise direction, $\delta t = 2\pi/100$, $\delta x = 0.01$, are adopted, whilst a non-uniform grid in the transverse direction has $\delta y = 0.03$ close to the axis of symmetry increasing to $\delta y = 0.8$ at the outer edge of the computational domain $y_{max} = 100$.

To implement the numerical scheme, we require an initial solution over the whole spatial domain $0 \leqslant x \leqslant 10$, $0 \leqslant y \leqslant 100$. This is achieved by setting $\epsilon = 0$ in (2.4) to determine what is essentially a steady-state solution consequent upon a steady uniform flow from the orifice. In doing so, we accommodate the singular behaviour implied

https://doi.org/10.1017/S0022112009991261 Published online by Cambridge University Press

by (2.4) at the lips $y=\pm 1$ by writing the onset flow at $x=0$ as

$$u_0(y)=\frac{1}{2}(1+\epsilon\cos t)\left[1-\tanh\left(\frac{y-1}{\delta}\right)\right], \qquad \delta=0.03.$$

With an initial solution in place, consider how this is now advanced in time. Suppose the solution is known up to some time $t=t_{n-1}$. The spatial integration commences at $x=0$, and following a suitable quasi-linearization of the momentum equation in (2.3), the following set of algebraic equations is to be solved

$$A_j(u^*, v^*)u\big|^n_{i,j+1}+B_j(u^*, v^*)u\big|^n_{i,j}+C_j(u^*, v^*)u\big|^n_{i,j-1}=D_j\left(u\big|^n_{i-1,j}, u^n_{i-2,j}, u^{n-1}_{i,j}, u^{n-2}_{i,j}\right), \tag{2.6}$$

with $i=1, \ldots, N_x$ and $j=1, \ldots, N_y$, where $N_x=1000$ and $N_y=500$ are the number of grid points in the x and y directions, respectively. The notation in (2.6) is such that $u|^n_{i,j}=u(x_i, y_j, t_n)$, $v|^n_{i,j}=v(x_i, y_j, t_n)$ and (u^*, v^*) are the best available estimates for the velocity components (u, v) at each grid point; so at each streamwise location we have the initial estimate $u^*_j=u|^n_{i-1,j}$, $v^*_j=v|^n_{i-1,j}$. The solution to the tridiagonal system (2.6), obtained using the Thomas algorithm, yields improved estimates of u and (from (2.3b)) v. These values are used to update u^* and v^*, and the iterative process continues until convergence is achieved. This is defined to be when $\sum_{j=1}^{N_y}|u^*_j-u^n_{i,j}|$ falls below a prescribed tolerance. The results have been checked for grid independence by comparison with results obtained with finer grids in sample calculations. The temporal integration continues until the solution has settled to a time-periodic state. The accuracy of the numerical results was tested by comparison with the integral constraint obtained from (2.3):

$$\int_0^\infty <u^2>\,\mathrm{d}y=1+\tfrac{1}{2}\epsilon^2, \quad \text{where} \quad <\cdot>=\frac{1}{2\pi}\int_0^{2\pi}.\,\mathrm{d}t. \tag{2.7}$$

Numerical solutions have been obtained, in particular, with $S=2$ for a range of values of ϵ, $0<\epsilon\leqslant 0.4$. In all cases, time dependence of the solutions, associated with the modulation at $x=0$, decays very rapidly in the axial direction and the steady jet that emerges assumes the form of the steady, self-similar, two-dimensional jet obtained analytically by Bickley (1937). This solution, where we introduce the stream function ψ such that $u=\partial\psi/\partial y$, $v=-\partial\psi/\partial x$, may be written as

$$\psi_b(x, y)=\left\{9\left(1+\tfrac{1}{2}\epsilon^2\right)(x+x_0)\right\}^{1/3}f(\eta), \quad \eta=\tfrac{1}{6}\left\{9\left(1+\tfrac{1}{2}\epsilon^2\right)\right\}^{1/3}(x+x_0)^{-2/3}y, \tag{2.8}$$

where $f(\eta)=\tanh\eta$ and the integral constraint (2.7), which expresses constancy of mean momentum flux, has been employed. The constant x_0, which can be expected to depend upon ϵ, fixes the position of the virtual origin of the Bickley solution.

To illustrate the rapid axial approach to a time-independent state, it is convenient to write

$$u(x, y, t)=u_0(x, y)+u_1(x, y, t),$$

where $|u_1|\ll|u_0|$ as $x\to\infty$. With the anticipated periodic form of the time-dependent part, we set

$$u_1(x, y, t)=u_{11}(x, y)\cos t+u_{12}(x, y)\sin t=\left(u^2_{11}+u^2_{12}\right)^{1/2}\cos(t+\phi), \tag{2.9}$$

where

$$u_{11}=\frac{1}{\pi}\int_0^{2\pi}u\cos t\,\mathrm{d}t, \qquad u_{12}=\frac{1}{\pi}\int_0^{2\pi}u\sin t\,\mathrm{d}t. \tag{2.10}$$

https://doi.org/10.1017/S0022112009991261 Published online by Cambridge University Press

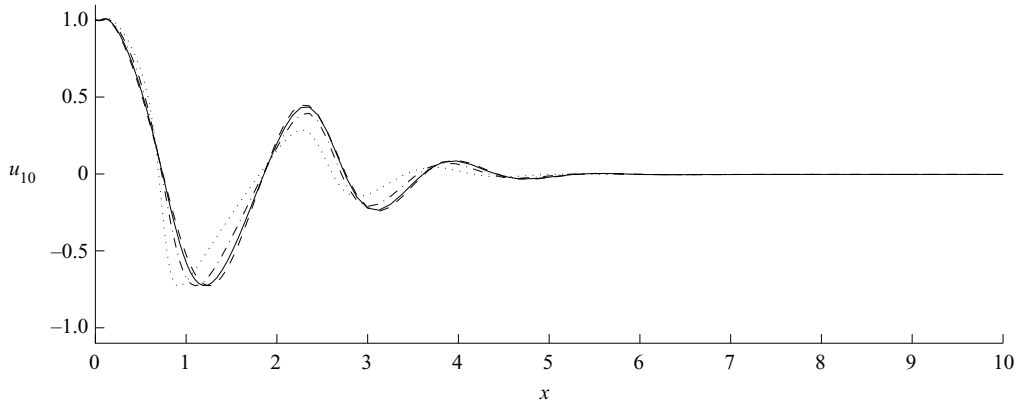


FIGURE 1. The normalized time-dependent centreline velocity $u_{10} = \{u(x, 0, t_m) - u_0(x, 0)\}/\epsilon$ for the case $S = 2$ with $\epsilon = 0.05$ (broken line); $\epsilon = 0.1$ (solid line); $\epsilon = 0.2$ (dot-dash line); $\epsilon = 0.4$ (dotted line).

In figure 1, we present, for the case $S = 2$ and various values of ϵ, the normalized time-dependent centreline velocity $u_{10} = \{u(x, 0, t) - u_0(x, 0)\}/\epsilon$, at a time t_m such that $\cos(t_m + \phi) = 1$. The rapid decay is evident; it is qualitatively similar for each value of ϵ and shows a decay rate greater than the algebraic decay associated with the Bickley jet. The results we have obtained for other values of S are qualitatively similar to those shown in figure 1 with an enhanced rate of decay as S increases.

We next investigate the nature of this rapid decay by means of a perturbation analysis for $\epsilon \ll 1$.

3. Asymptotic theory

It is convenient to write the governing equations (2.3) in terms of the stream function ψ as

$$S\frac{\partial u}{\partial t} + \frac{\partial(u, \psi)}{\partial(x, y)} = \frac{\partial^2 u}{\partial y^2}, \qquad u = \frac{\partial \psi}{\partial y}. \tag{3.1}$$

The onset conditions at $x = 0$ are as in (2.4) together with

$$\left.\begin{aligned} &\psi = \partial u/\partial y = 0 \quad \text{at} \quad y = 0, \quad x > 0, \\ &u \to 0 \quad \text{as} \quad y \to \infty, \quad x > 0. \end{aligned}\right\} \tag{3.2}$$

With the assumption that $\epsilon \ll 1$, we expand ψ, u as

$$\left.\begin{aligned} &\psi = \psi_0 + \tfrac{1}{2}\epsilon(\psi_1 \mathrm{e}^{\mathrm{i}t} + \bar{\psi}_1 \mathrm{e}^{-\mathrm{i}t}) + O(\epsilon^2), \\ &u = u_0 + \tfrac{1}{2}\epsilon(u_1 \mathrm{e}^{\mathrm{i}t} + \bar{u}_1 \mathrm{e}^{-\mathrm{i}t}) + O(\epsilon^2). \end{aligned}\right\} \tag{3.3}$$

Substitution into (3.1) then gives, at $O(1)$,

$$\frac{\partial(u_0, \psi_0)}{\partial(x, y)} = \frac{\partial^2 u_0}{\partial y^2}, \qquad u_0 = \frac{\partial \psi_0}{\partial y}, \tag{3.4}$$

with, at $x = 0$,

$$u_0 = \begin{cases} 1, & |y| < 1, \\ 0, & |y| > 1, \end{cases}$$

https://doi.org/10.1017/S0022112009991261 Published online by Cambridge University Press

together with

$$\psi_0 = \partial u_0/\partial y = 0 \quad \text{at} \quad y = 0, \quad x > 0,$$
$$u_0 \to 0 \quad \text{as} \quad y \to \infty, \quad x > 0,$$

At $O(\epsilon)$,

$$\mathrm{i}Su_1 + \frac{\partial(u_0, \psi_1)}{\partial(x, y)} + \frac{\partial(u_1, \psi_0)}{\partial(x, y)} = \frac{\partial^2 u_1}{\partial y^2}, \qquad u_1 = \frac{\partial \psi_1}{\partial y}, \tag{3.5}$$

with, at $x = 0$,

$$u_1 = \begin{cases} 1, & |y| < 1, \\ 0, & |y| > 1, \end{cases}$$

together with

$$\psi_1 = \partial u_1/\partial y = 0, \quad \text{at} \quad y = 0, \quad x > 0,$$
$$u_1 \to 0 \quad \text{as} \quad y \to \infty, \quad x > 0.$$

When x is sufficiently large for (2.8), with $\epsilon = 0$, to be a valid approximation, the $O(\epsilon)$ perturbation can be expressed as

$$\psi_1 = \{9(x + x_0)\}^{1/3} F(\xi, \eta), \tag{3.6}$$

where

$$\xi = \tfrac{4}{9} S\{9(x + x_0)\}^{4/3}, \tag{3.7}$$

and from (3.5)

$$F_{\eta\eta\eta} + 2(fF_{\eta\eta} + 2f'F_\eta + f''F) + 8\xi(f''F_\xi - f'F_{\xi\eta}) - \mathrm{i}\xi F_\eta = 0. \tag{3.8}$$

The boundary conditions on $F(\xi, \eta)$ are that

$$\left.\begin{aligned} F = F_{\eta\eta} = 0 \quad &\text{at} \quad \eta = 0, \\ \text{and} \qquad F_\eta \to 0 \quad &\text{as} \quad \eta \to \infty. \end{aligned}\right\}$$

Equation (3.8) can also be put in the form

$$G_{\eta\eta} - 8f'\xi G_\xi - \mathrm{i}\xi F_\eta = 0, \qquad G(\xi, \eta) = F_\eta + 2fF.$$

The equation for $F(\xi, \eta)$ has an exact solution

$$F(\xi, \eta) = X(\xi) - \mathrm{i}Y(\xi) f'(\eta), \tag{3.9}$$

and hence

$$G(\xi, \eta) = 2X(\xi) f(\eta),$$

provided that

$$Y(\xi) = 8X'(\xi) + 2\xi^{-1} X(\xi). \tag{3.10}$$

This can be only an outer solution of the full problem, because $F(\xi, \eta)$ in (3.9) is not an odd function of η. It may be noted that, for fixed ξ, this outer solution makes

$$u_1 = -\left(\frac{\xi}{S}\right)^{1/2} \mathrm{i}Y(\xi) \frac{\partial u_0}{\partial y}.$$

Some insight into the behaviour of $X(\xi)$ may be gained by integrating (3.8) to give

$$\mathrm{i}F(\xi, \infty) = 16 \frac{\mathrm{d}}{\mathrm{d}\xi} \int_0^\infty f''(\eta) F(\xi, \eta)\, \mathrm{d}\eta.$$

https://doi.org/10.1017/S0022112009991261 Published online by Cambridge University Press

The form of the outer solution, from (3.9) and (3.10), is

$$F(\xi,\eta)=X(\xi)-\mathrm{i}\{8X'(\xi)+2\xi^{-1}X(\xi)\}f'(\eta),$$

and substitution of this into the above integral yields an equation for X. This, of course, neglects any contribution to the integral from an inner solution, but that may be expected to be small since $f''=F=0$ at $\eta=0$. The resulting equation for $X(\xi)$ is

$$X''(\xi)+\tfrac{1}{4}(\mathrm{i}+\xi^{-1})X'(\xi)-\left(\tfrac{1}{64}+\tfrac{1}{4}\xi^{-2}\right)X(\xi)=0. \tag{3.11}$$

Equation (3.11) has solutions of the form

$$X(\xi)\sim A\exp\left\{-\tfrac{1}{8}\mathrm{i}\xi\pm\tfrac{1}{4}(1+\mathrm{i})\xi^{1/2}\right\}\xi^{1/8},$$

as $\xi\to\infty$. As remarked, in obtaining this result the inner region has been neglected, but it does motivate a structure of the outer solution in the form

$$X(\xi)\sim A\exp\left(\lambda\xi+\mu\xi^{1/2}\right)\xi^{k},$$

and it is plausible that $\lambda=-\frac{1}{8}\mathrm{i}$.

Guided by this, we seek an inner solution in the form

$$F(\xi,\eta)=\exp\left(\lambda\xi+\mu\xi^{1/2}\right)\xi^{k}\left\{f_0(z)+\xi^{-1/2}f_1(z)+\cdots\right\},$$

where z is a suitable inner variable. Details of the construction of the inner solution are given in the Appendix; here we present only an outline. It appears to be impossible to match with the outer solution unless

$$\lambda=-\tfrac{1}{8}\mathrm{i},$$

and that the matching condition on $f_0(z)$ is then an eigenvalue problem for μ, with the solution

$$\mu=\left(\tfrac{1}{4}-n\right)\sqrt{\mathrm{i}},\quad n=0,1,2,\ldots.$$

The numerical solution indicates that $F(\xi,\eta)$ decays exponentially as $\xi\to\infty$, so we assume that the case $n=0$ is absent. The dominant solution is therefore that with

$$\mu=-\tfrac{3}{4}\sqrt{\mathrm{i}}.$$

For each eigenvalue μ, the corresponding value of k comes from the equation for $f_1(z)$: the case $\mu=-\frac{3}{4}\sqrt{\mathrm{i}}$ requires

$$k=-\tfrac{3}{4}.$$

Note that $f_1(z)$ contains an arbitrary multiple of $f_0(z)$, which has to be found from the equation for $f_2(z)$.

The solution of the equations gives the centreline speed from

$$F_\eta(\xi,0)=-4AE(\xi)(\mathrm{i}\xi)^{-1/2}\left\{1+\tfrac{3}{16}(\mathrm{i}\xi)^{-1/2}+O(\xi^{-1})\right\}, \tag{3.12}$$

where

$$E(\xi)=\exp\left\{-\tfrac{1}{8}\mathrm{i}\xi-\tfrac{3}{4}(\mathrm{i}\xi)^{1/2}\right\},$$

and A is a complex constant. Matching with the outer solution yields

$$F(\xi,\infty)=X(\xi)=\sqrt{2\pi}AE(\xi)(\mathrm{i}\xi)^{-1/4}\left\{1+\tfrac{39}{16}(\mathrm{i}\xi)^{-1/2}+O(\xi^{-1})\right\} \tag{3.13}$$

and

$$\mathrm{i}Y(\xi)=\sqrt{2\pi}AE(\xi)(\mathrm{i}\xi)^{-1/4}\left\{1+\tfrac{87}{16}(\mathrm{i}\xi)^{-1/2}+O(\xi^{-1})\right\}.$$

https://doi.org/10.1017/S0022112009991261 Published online by Cambridge University Press

Furthermore, it is perhaps worth noting that (3.12) shows the decay of the perturbation centreline velocity to be exponential, unlike the algebraic decay of the corresponding time-averaged velocity.

4. A comparison between the asymptotic and numerical results

Initially, we integrated the analogues of (3.4) and (3.5) for the velocity components (u_0, v_0) and (u_1, v_1) by the numerical method used for (2.3). The time-independent part (u_0, v_0) eventually develops into the self-similar form of Bickley ((2.8) with $\epsilon = 0$) in which, for example, the streamwise centreline speed decays algebraically, as $O(x^{-1/3})$, as $x \to \infty$. Unsurprisingly, perhaps, the perturbation solution (u_1, v_1) does not decay, but grows exponentially as $x \to \infty$. This growing eigensolution is consistent with the lowest eigenvalue $\mu_0 = \frac{1}{4}\sqrt{\mathrm{i}}$ recorded in § 3. However, the solutions we have obtained of the nonlinear problem (2.3) to (2.5) indicate that this eigensolution is spurious and may be neglected.

Secured in the knowledge from the calculations described in § 2 that the time-dependent element of the solution decays more rapidly than the time-independent part, a comparison with the asymptotic solution of § 3 is appropriate. As for the velocity component $u(x, y, t)$ in (2.9), we write the stream function ψ as

$$\psi(x, y, t) = \psi_0(x, y) + \psi_1(x, y, t), \tag{4.1}$$

Again, with the anticipated form of the time-dependent part, we set

$$\psi_1(x, y, t) = \psi_{11}(x, y)\cos t + \psi_{12}(x, y)\sin t = \left(\psi_{11}^2 + \psi_{12}^2\right)^{1/2}\cos(t + \theta), \tag{4.2}$$

where

$$\psi_{11} = \frac{1}{\pi}\int_0^{2\pi} \psi \cos t \, \mathrm{d}t, \qquad \psi_{12} = \frac{1}{\pi}\int_0^{2\pi} \psi \sin t \, \mathrm{d}t. \tag{4.3}$$

In order to make a meaningful comparison with the asymptotic solution, we require a solution of the nonlinear problem for small ϵ, and we have chosen $\epsilon = 0.05$. As noted in § 2, the classical solution of Bickley (1937) emerges as $x \to \infty$, with a virtual origin at $x = -x_0(\epsilon)$, as $u_0(x, y) \sim \frac{1}{6}\{9(1 + \frac{1}{2}\epsilon^2)\}^{2/3}(x + x_0)^{-1/3}\mathrm{sech}^2\eta$. The quantity x_0 can therefore be estimated as $x_0 = \lim_{x\to\infty}[3(1 + \frac{1}{2}\epsilon^2)^2\{2u_0(x, 0)\}^{-3} - x]$ from which we find, for $\epsilon = 0.05$, $x_0 = 0.207$.

In figures 2–4, we show the time-dependent centreline velocity and the stream function at the edge of the jet. The rapid decay is evident and, furthermore, we see that the decay rate increases as S increases, consistent with (3.7), (3.12) and (3.13).

To investigate further the relationship between the numerical results and the asymptotic theory of § 3, first define a quantity R as

$$R = \left(\frac{\psi_{11}^2(x, y_{max}) + \psi_{12}^2(x, y_{max})}{u_{11}^2(x, 0) + u_{12}^2(x, 0)}\right)^{1/2}. \tag{4.4}$$

In figure 4, we show $RS^{-1/4}(x + x_0)^{-1}$ as a function of x which, in all cases, approaches a constant value. From the inner and outer solutions, as in (3.12) and (3.13), we see that $|\psi_1(x, \infty, t)/u_1(x, 0, t)|S^{-1/4}(x + x_0)^{-1} \to 3.07$ as $x \to \infty$, which is slightly higher than the values recorded by the numerical calculations. Finally, in figure 6, we show the phase differences (see (2.9) and (4.2)) between the outer and inner solutions $\theta - \phi$. The asymptotic theory (see (3.12) and (3.13)) shows that as $x \to \infty$, $\theta - \phi \to \pi/8$, which is slightly lower than the value predicted by the numerical calculations.

https://doi.org/10.1017/S0022112009991261 Published online by Cambridge University Press

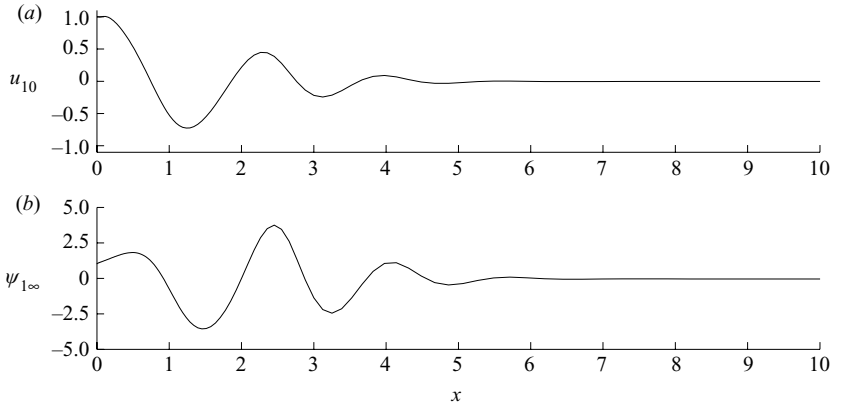


FIGURE 2. (*a*) The normalized, time-dependent centreline velocity, $u_{10} = \{u(x, 0, t) - u_0(x, 0)\}/\epsilon$ and (*b*) the corresponding stream function at the edge of the jet, $\psi_{1\infty} = \{\psi(x, y_{max}, t) - \psi_0(x, y_{max}\}/\epsilon$, with $S = 2$ at a time t such that $\cos t = 1$. In the numerical calculation $\epsilon = 0.05$.

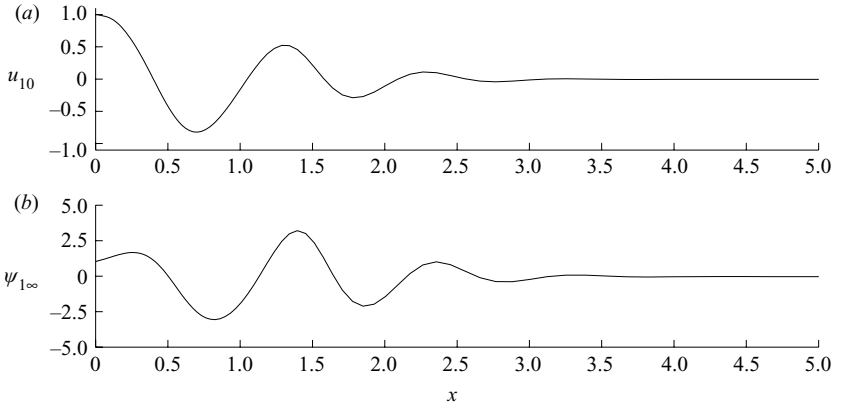


FIGURE 3. Same as for figure 2 with $S = 4$.

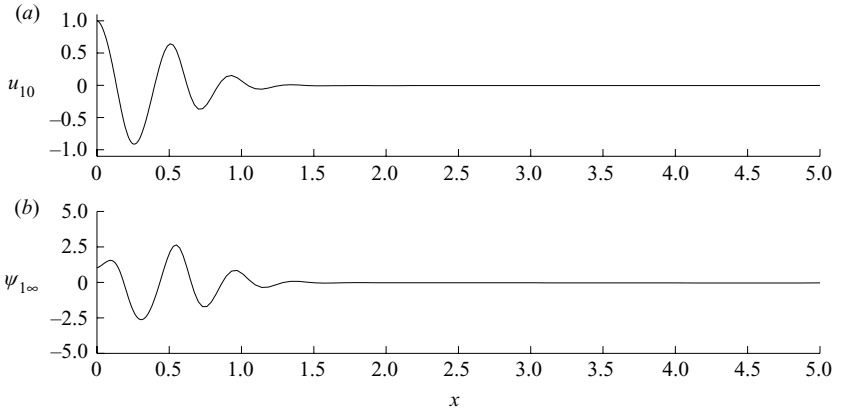


FIGURE 4. Same as for figure 2 with $S = 12$.

https://doi.org/10.1017/S0022112009991261 Published online by Cambridge University Press

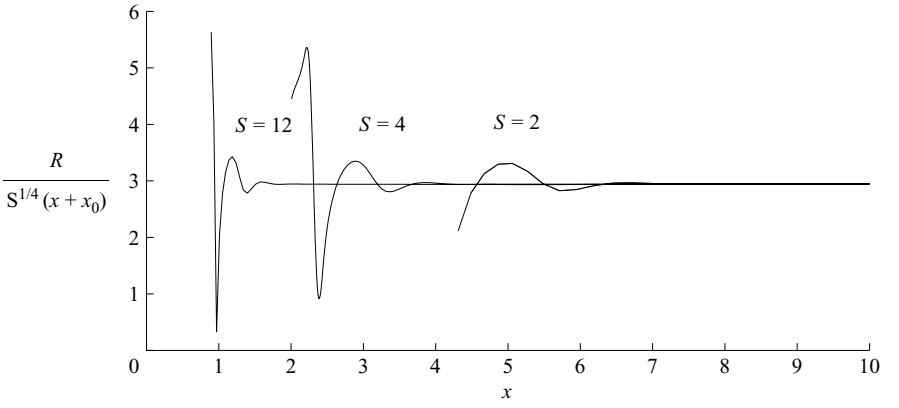


FIGURE 5. Quantity $R(x+x_0)^{-1}S^{-\frac{1}{4}}$, with R as in (4.4), for values of $S=12$, 4 and 2.

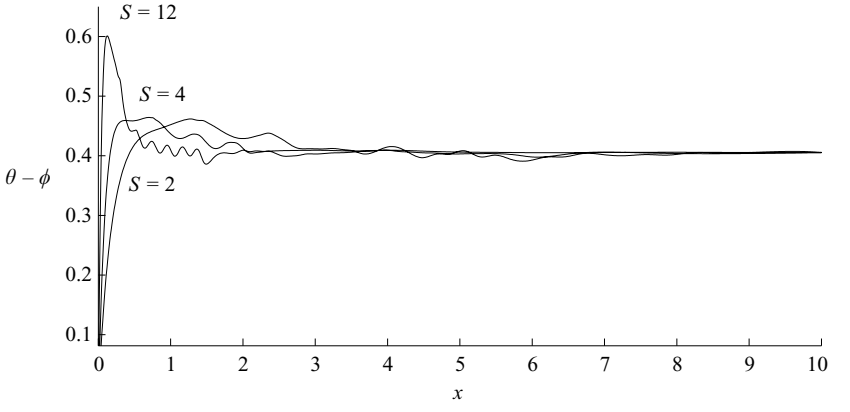


FIGURE 6. Phase difference between u_{10} and $\psi_{1\infty}$ for $S=12$, 4 and 2.

The small differences that have been noted in figures 5 and 6 between the asymptotic analysis and the numerical calculations may be attributed to the fact that in the analysis terms $O(\epsilon^2)$ have not been considered.

5. Conclusions

In this paper, we have analysed the structure of a plane jet that is discharged from between plane boundaries into an ambient atmosphere. The onset flow at the orifice has a prescribed steady component upon which a time-dependent harmonic fluctuation is superposed. Asymptotic analysis and numerical calculations, in which marching in time and axial distance yields a time-periodic solution, show that the time-dependent part of the solution decays exponentially with downstream axial distance. By contrast, the time-averaged solution decays more slowly, developing into the well-known Bickley (1937) jet that decays algebraically with axial distance.

M. S.-S. acknowledges the support of the Spanish MEC under projects # ENE2005-08580-C02-01 and # ENE2005-09190-CO4-01 and the regional government of Comunidad de Madrid under project S-505/ENE/0229 during the period in which this work was carried out.

https://doi.org/10.1017/S0022112009991261 Published online by Cambridge University Press

Appendix. The inner expansion

The inner solution is sought in the form

$$F(\xi,\eta)=\exp\left(\lambda\xi+\mu\xi^{1/2}\right)\xi^{k}\left\{f_0(z)+\xi^{-1/2}f_1(z)+\xi^{-1}f_2(z)+\cdots\right\}, \tag{A 1}$$

where z is a suitable inner variable. The natural choice is

$$z=\xi^{1/2}\eta=S^{1/2}y.$$

From (3.8), this choice leads to

$$f_0'''-(8\lambda+\mathrm{i})f_0'=0.$$

If $\lambda\neq-\frac{1}{8}\mathrm{i}$, then

$$f_0(z)=A\sin\{(8\lambda+\mathrm{i})^{1/2}z\},$$

since $f_0(z)$ is an odd function and $f_1(z)$, $f_2(z)$, ... consist of functions $\cos\{(8\lambda+\mathrm{i})^{1/2}z\}$ and $\sin\{(8\lambda+\mathrm{i})^{1/2}z\}$ multiplied by polynomials in z, it seems impossible to match this expansion with the outer solution. If $\lambda=-\frac{1}{8}\mathrm{i}$, then

$$f_0(z)=Az,$$

and $f_n(z)$ is an odd polynomial of degree $(2n+1)$ in z. This indicates that the appropriate inner variable is $\xi^{-1/4}z=\xi^{1/4}\eta$ which, in turn, implies that the thickness of this inner region is $O((x+x_0)^{1/3})$, whereas the thickness of the main jet region is $O((x+x_0)^{2/3})$.

It is easier to develop the inner solution in terms of $f(\eta)$ rather than η and, to avoid the repeated occurrence of $\sqrt{\mathrm{i}}$, it is more convenient to work with the variables

$$s=(\mathrm{i}\xi)^{1/2},\quad \zeta=(\mathrm{i}\xi)^{1/2}f^2(\eta).$$

In terms of these variables, (3.8) becomes

$$4(s-\zeta)^2\zeta F_{\zeta\zeta\zeta}+6(s-\zeta)(s-3\zeta)F_{\zeta\zeta}-(s^3+6s-2\zeta)F_\zeta-2F-4s\{(s-\zeta)F_{s\zeta}+F_s\}=0.$$

On differentiation

$$4(s-\zeta)^2\zeta F_{\zeta\zeta\zeta\zeta}+10(s-\zeta)(s-3\zeta)F_{\zeta\zeta\zeta}-(s^3+30s-38\zeta)F_{\zeta\zeta}-4s(s-\zeta)F_{s\zeta\zeta}=0.$$

Then if

$$F_{\zeta\zeta}=\exp(-\tfrac{1}{8}s^2-as-b\log s)\Phi(s,\zeta),$$

where a and b correspond to μ and k in (A1), $\Phi(s,\zeta)$ satisfies

$$4(s-\zeta)^2\zeta\Phi_{\zeta\zeta}+10(s-\zeta)(s-3\zeta)\Phi_\zeta+$$
$$+\{4as^2+(4b-30)s-(s^2+4as+4b-38)\zeta\}\Phi-4s(s-\zeta)\Phi_s=0.$$

We now expand $\Phi(s,\zeta)$ as

$$\Phi(s,\zeta)=\phi_0(\zeta)+s^{-1}\phi_1(\zeta)+s^{-2}\phi_2(\zeta)+\cdots, \tag{A 2}$$

where the condition that $F(\xi,\eta)$ is an odd function of η implies that

$$\phi_n(\zeta)=\zeta^{-3/2}\times\text{power series in }\zeta.$$

The leading term of (A2) is given by

$$4\zeta\phi_0''+10\phi_0'+(4a-\zeta)\phi_0=0, \tag{A 3}$$

and the required solution is

$$\phi_0(\zeta)=A\mathrm{e}^{-1/2\zeta}\zeta^{-3/2}{}_1F_1\left(-a-\tfrac{1}{4};-\tfrac{1}{2};\zeta\right),$$

https://doi.org/10.1017/S0022112009991261 Published online by Cambridge University Press

where A is a complex constant. As $\mathscr{R}(\zeta)\to+\infty$, $\phi_0(\zeta)$ is exponentially large unless the series for the confluent hypergeometric function ${}_1F_1$ terminates. In order to be able to match, we therefore have an eigenvalue problem with the solution

$$a+\tfrac{1}{4}=0,1,2,\ldots.$$

The numerical solution of the original equations indicates that $F(\xi,\eta)$ is exponentially small as $\xi\to\infty$, so we assume that the eigenvalue $a=-\frac{1}{4}$ is absent. In the following, we take

$$a=\tfrac{3}{4},$$

since this is expected to be the dominant case, and therefore

$$\phi_0(\zeta)=A\mathrm{e}^{-1/2\zeta}\zeta^{-3/2}(1+2\zeta),$$

and similar calculations can be made with the other eigenvalues.

The equation for $\phi_1(\zeta)$ is now

$$4\zeta\phi_1''+10\phi_1'+(3-\zeta)\phi_1=8\zeta^2\phi_0''+40\zeta\phi_0'+(30-4b+3\zeta)\phi_0, \tag{A 4}$$

and the substitution

$$\phi_1(\zeta)=A\mathrm{e}^{-1/2\zeta}\zeta^{-3/2}\chi_1(\zeta)$$

leads to

$$4\zeta\chi_1''-(4\zeta+2)\chi_1'+4\chi_1=-4b+(27-8b)\zeta-24\zeta^2+4\zeta^3.$$

Unless $\chi_1(\zeta)$ is a polynomial, it becomes large as $\zeta\to\infty$ like $\zeta^{-1/2}\mathrm{e}^{\zeta}$ and makes $\phi_1(\zeta)$ exponentially great. In this way, we find that

$$b=\tfrac{3}{2}$$

and

$$\chi_1(\zeta)=c_1(1+2\zeta)+3\zeta+\tfrac{15}{4}\zeta^2-\tfrac{1}{2}\zeta^3,$$

where c_1 is an arbitrary constant, corresponding to the fact that $\phi_0(\zeta)$ is a complementary function of (A4).

The constant c_1 is determined by the condition that $\phi_2(\zeta)$ is not large at infinity. The equation for $\phi_2(\zeta)$, on making use of (A3) and (A4), is

$$4\zeta\phi_2''+10\phi_2'+(3-\zeta)\phi_2=20\zeta\phi_1'+(20-3\zeta+2\zeta^2)\phi_1+20\zeta^2\phi_0'+(16\zeta-3\zeta^2+3\zeta^3)\phi_0.$$

Then if

$$\phi_2(\zeta)=A\mathrm{e}^{-1/2\zeta}\zeta^{-3/2}\chi_2(\zeta),$$

we have, for $\chi_2(\zeta)$,

$$4\zeta\chi_2''-(4\zeta+2)\chi_2'+4\chi_2=c_1(4\zeta^3-24\zeta^2+7\zeta-10)-\zeta^5+20\zeta^4-\tfrac{363}{4}\zeta^3+\tfrac{145}{2}\zeta^2+16\zeta.$$

As with $\chi_1(\zeta)$, $\chi_2(\zeta)$ must be a polynomial and this leads to

$$c_1=\tfrac{3}{16},$$

and so

$$\chi_1(\zeta)=\tfrac{3}{16}+\tfrac{27}{8}\zeta+\tfrac{15}{4}\zeta^2-\tfrac{1}{2}\zeta^3.$$

Thus, from the dominant eigenvalue $a=\frac{3}{4}$, we have the inner expansion

$$F(\xi,\eta)=E(\xi)(\mathrm{i}\xi)^{-3/4}\{F_0(\zeta)+(\mathrm{i}\xi)^{-1/2}F_1(\zeta)+\cdots\},$$

https://doi.org/10.1017/S0022112009991261 Published online by Cambridge University Press

where

$$E(\xi) = \exp\left\{-\tfrac{1}{8}\mathrm{i}\xi - \tfrac{3}{4}(\mathrm{i}\xi)^{1/2}\right\},$$

and

$$F_n''(\zeta) = \phi_n(\zeta).$$

Since $F_n(\zeta) = \zeta^{1/2} \times$ power series in ζ,

$$F_0(\zeta) = A\left\{2\mathrm{e}^{-1/2\zeta}\zeta^{1/2} + (\zeta - 3)\int_0^\zeta t^{-1/2}\mathrm{e}^{-1/2t}\,\mathrm{d}t\right\},$$
$$F_1(\zeta) = A\left\{\mathrm{e}^{-1/2\zeta}\left(\tfrac{111}{8}\zeta^{1/2} - 2\zeta^{3/2}\right) + \left(\tfrac{87}{16}\zeta - \tfrac{117}{16}\right)\int_0^\zeta t^{-1/2}\mathrm{e}^{-1/2t}\,\mathrm{d}t\right\}.$$

As $\zeta \to 0$,

$$F_0(\zeta) = -4A\zeta^{1/2} + O\left(\zeta^{3/2}\right),$$
$$F_1(\zeta) = -\tfrac{3}{4}A\zeta^{1/2} + O\left(\zeta^{3/2}\right),$$

and as $\zeta \to \infty$,

$$F_0(\zeta) = A\sqrt{2\pi}(\zeta - 3) + \text{exp. small},$$
$$F_1(\zeta) = A\sqrt{2\pi}\left(\tfrac{87}{16}\zeta - \tfrac{117}{16}\right) + \text{exp. small}.$$

From these results, it follows that

$$F_\eta(\xi, 0) = AE(\xi)(\mathrm{i}\xi)^{-1/2}\left\{-4 - \tfrac{3}{4}(\mathrm{i}\xi)^{-1/2} + O(\xi^{-1})\right\},$$

and as $\zeta \to \infty$

$$F(\xi, \eta) = A\sqrt{2\pi}E(\xi)(\mathrm{i}\xi)^{-3/4}\left\{\zeta - 3 + \left(\tfrac{87}{16}\zeta - \tfrac{117}{16}\right)(\mathrm{i}\xi)^{-1/2} + O(\xi^{-1})\right\},$$

so that in terms of $f(\eta)$,

$$F(\xi, \eta) \sim A\sqrt{2\pi}E(\xi)(\mathrm{i}\xi)^{-3/4}\left\{(\mathrm{i}\xi)^{1/2}f^2(\eta) - 3 + \tfrac{87}{16}f^2(\eta) - \tfrac{117}{16}(\mathrm{i}\xi)^{-1/2} + \cdots\right\}. \quad \text{(A 5)}$$

Matching (A5) to

$$F(\xi, \eta) = X(\xi) - \mathrm{i}Y(\xi)f'(\eta) = X(\xi) - \mathrm{i}Y(\xi) + \mathrm{i}Y(\xi)f^2(\eta)$$

gives

$$X(\xi) = A\sqrt{2\pi}E(\xi)(\mathrm{i}\xi)^{-1/4}\left\{1 + \tfrac{39}{16}(\mathrm{i}\xi)^{-1/2} + \cdots\right\},$$
$$\mathrm{i}Y(\xi) = A\sqrt{2\pi}E(\xi)(\mathrm{i}\xi)^{-1/4}\left\{1 + \tfrac{87}{16}(\mathrm{i}\xi)^{-1/2} + \cdots\right\}.$$

REFERENCES

BICKLEY, W. G. 1937 The plane jet. *Phil. Mag.* **23**, 727–731.
SCHLICHTING, H. 1933 Laminare Strahlausbreitung. *Z. angew. Math. Mech.* **13**, 260–263.

https://doi.org/10.1017/S0022112009991261 Published online by Cambridge University Press